

An ab Initio Investigation of the Ground and First Two Excited Electronic States of the Difluoromethyl Radical

Peter S. Fudacz, Janell D. Dober, Dennis L. Jarman, Jean M. Standard,* and Robert W. Quandt*

Department of Chemistry, Illinois State University, Normal, Illinois 61790-4160

Received: August 13, 2003; In Final Form: September 9, 2003

Ab initio calculations have been performed to determine the structure and energies of the ground and first two excited electronic states of CHF₂. The 6-31+G*, 6-311++G**, aug-ccpVDZ, and aug-cc-pVTZ basis sets were utilized at the MP2 and CCSD(T) levels of theory for the structures and energies of minima and transition states on the ground electronic surface. The 6-31+G*, 6-311++G** basis sets were utilized at the CIS, CASSCF, and MRCI levels of theory for characterization of the excited electronic states. The ground state was found to be pyramidal, the first excited state is possibly dissociative and the second excited state planar. Vertical transition energies for transitions from the ground to the first and second excited states were found to range from 61 355 to 71 372 cm⁻¹ at the CIS level of theory. Shallow local minima on the \tilde{A} state potential energy surface with long C–H bonds of about 2.0 Å were located by using two-dimensional potential surface scans. Upon excitation to the \tilde{B} state, the C–H bond stays constant near 1.08 Å, the C–F bond lengthens from 1.33 to 1.45 Å, the H–C–F bond angle increases from 114° to 133°, and the F–C–F angle decreases from 110° to 93°.

I. Introduction

The photodissociation of halocarbons in general, and chlorofluorocarbons (CFCs) in specific, has received much interest due to the role these species play in stratospheric ozone depletion and as greenhouse gases.¹ Alternatives to CFCs that are currently in use include hydrochlorofluorocarbons (HCFCs) and hydrofluorocarbons (HFCs). These replacement species are oxidized relatively quickly by OH radicals in the troposphere, giving them an atmospheric lifetime on the order of 1 to 12 years. Despite this short lifetime, a small percentage of these HCFCs can reach the upper atmosphere. This was demonstrated by measurements taken during the ATLAS-3 mission in 1994. These measurements showed dramatic increases in the amount of HCFC-22 (CHF₂Cl) in the stratosphere compared to previous missions.²

The principal photoproduct from the UV photolysis of CHF₂Cl is generally CHF₂. In addition to its increasing importance in stratospheric chemistry, CHF₂ has also been identified as an important intermediate from the reaction of hydrogen atoms with halons in the flame suppression process^{3,4} and secondary reactions of fluorine- and chlorine-substituted methyl radicals.⁵ In addition, the question of whether the ground states of methyl and halomethyl radicals have planar or pyramidal geometries has long been of interest to theorists and spectroscopists.^{6–15}

To date most of the experimental work on CHF₂ has been limited to microwave or infrared spectroscopic studies of the ground state. In addition, almost all of the theoretical work has focused on either the ground-state structure or reaction mechanisms with various atmospherically important radicals. The key exception has been the work of Dearden et al.¹⁶ In their study the ground and several excited states of CHF₂ were investigated theoretically at the UHF and UMP2 levels of theory with the 6-31* and 6-31G** basis sets and experimentally by using resonance-enhanced multiphoton ionization (REMPI) spectroscopy. The equilibrium geometry of CHF₂ on the ground electronic surface was determined by Dearden et al. to be

nonplanar (*C_s* symmetry). In addition to the equilibrium structure, a planar transition state for inversion (with *C_{2v}* symmetry) was located on the ground electronic surface as well as on the \tilde{A} and \tilde{E} excited electronic states. Because they were using perturbation theory, Dearden et al. were unable to calculate the properties of any state with the same symmetry as the ground-state such as the \tilde{B} , \tilde{C} , and \tilde{D} states. In addition, their results indicate that the \tilde{A} excited state transition structure has a physically unrealistic carbon–hydrogen bond length of 3.98 Å. This erroneous result is not surprising in light of their use of perturbation theory and a double- ζ basis set in order to calculate excited-state parameters.

To refine the structure and properties of the ground electronic state and to further investigate the structures, transition energies, and potential surfaces of the excited electronic states for subsequent experimental studies, we have extended the computational work of Dearden et al. In this work we report the structures and energies of the ground and first two excited electronic states of CHF₂ using MP2, CCSD(T), CIS, CASSCF, and MRCI methods with double- and triple- ζ quality basis sets.

II. Methods

The structures, energies, and vibrational frequencies for both the global minimum and transition state for pyramidal inversion on the ground electronic surface were calculated at the MP2 and CCSD(T) levels of theory with the 6-31+G*, 6-311++G**, aug-cc-pVDZ, and aug-cc-pVTZ basis sets. The frozen core approximation was utilized in all the MP2 and CCSD(T) calculations.

Vertical excitation energies for the first three excited states were calculated by using the configuration interaction singles (CIS) method with 6-31+G* and 6-311++G** basis sets. Potential surface scans along the C–H coordinate for the ground and first three excited states of CHF₂ were also carried out using the CIS level of theory.

TABLE 1: Results for the Equilibrium Geometry and Transition State for Pyramidal Inversion on the Ground Electronic Surface of CHF₂ Using Various Basis Sets at the MP2 Level of Theory

coordinate	MP2				
	6-31G* ^a	6-31+G*	6-311++G**	aug-cc-pVDZ	aug-cc-pVTZ
Ground State					
<i>r</i> (H–C), Å	1.0882	1.0873	1.0876	1.0963	1.0844
<i>r</i> (C–F), Å	1.3368	1.3445	1.3294	1.3466	1.3275
θ (H–C–F), deg	113.68	113.46	113.81	113.78	113.94
θ (F–C–F), deg	111.44	110.90	111.18	110.81	111.01
dihedral, deg	N. A.	127.77	128.78	128.19	128.79
G. S. Transition Structure					
<i>r</i> (H–C), Å	1.0718	1.0727	1.0705	1.0785	1.0672
<i>r</i> (C–F), Å	1.3304	1.3359	1.3214	1.3368	1.3192
θ (H–C–F), deg	122.34	122.72	122.78	122.88	122.86
inversion barrier, cm ⁻¹ ^b	3176	2844	2542	2605	2438

^a MP2(Full) results from Dearden et al.¹⁶ ^b Reported values include vibrational zero-point energy corrections.

TABLE 2: Results for the Equilibrium Geometry and Transition State for Pyramidal Inversion on the Ground Electronic Surface of CHF₂ Using Various Basis Sets at the CCSD(T) Level of Theory

coordinate	CCSD(T)			
	6-31+G*	6-311++G**	aug-cc-pVDZ	aug-cc-pVTZ
Ground State				
<i>r</i> (H–C), Å	1.0915	1.0911	1.1003	1.0869
<i>r</i> (C–F), Å	1.3458	1.3318	1.3489	1.3291
θ (H–C–F), deg	113.59	113.93	113.91	114.07
θ (F–C–F), deg	110.90	111.18	110.72	110.88
dihedral, deg	127.87	128.84	128.31	128.84
G. S. Transition Structure				
<i>r</i> (H–C), Å	1.0782	1.0754	1.0838	1.0716
<i>r</i> (C–F), Å	1.3382	1.3247	1.3401	1.3215
θ (H–C–F), deg	122.75	122.80	122.89	122.89
inversion barrier, cm ⁻¹ ^a	2548	2289	2338	2210 ^b

^a Reported values include vibrational zero-point energy corrections. ^b The vibrational zero-point energy computed at the CCSD(T)/aug-cc-pVDZ level was used to correct the CCSD(T)/aug-cc-pVTZ inversion barrier.

The main configuration of the ground electronic state of CHF₂ is (core)3*a*'² 2*a*''² 4*a*'² 5*a*'² 3*a*''² 6*a*'² 4*a*''² 5*a*''² 7*a*'² 8*a*'¹. The core includes the 1*s* orbitals of the carbon and two fluorine atoms. The highest occupied orbital of the ground electronic state, 8*a*', corresponds to an orbital with C–F π^* antibonding character. To further characterize the excited electronic states, calculations were performed using the complete active space self-consistent field method with 19 valence electrons and 13 active orbitals, CASSCF(19,13). The 10 occupied valence orbitals of the main configuration of the ground electronic state (six with *a*' symmetry and four with *a*'' symmetry) were included in the CASSCF calculations along with the lowest three unoccupied orbitals (two with *a*' symmetry and one with *a*'' symmetry). For electronic states of CHF₂ with *A*' symmetry in the *C_s* point group, such as the ground and first excited state, this corresponds to the inclusion of 51 112 configuration state functions (CSFs) in the calculation. For states with *A*'' symmetry, such as the second excited state, 51 992 CSFs are included in the calculation. Geometry optimizations were attempted on both excited-state surfaces. In addition, two-dimensional potential surface scans using the CASSCF(19,13) method and the 6-31+G* or 6-311++G** basis sets were carried out for the first two excited states of CHF₂. Scans were performed in which the C–H distance and out-of-plane dihedral angle were varied, as well as scans in which the H–C–F and out-of-plane dihedral angles were varied. Selected scans and geometry optimizations were also performed using the multi-reference configuration interaction method with three electrons in four active orbitals, MRCI(3,4).

All of the MP2, CCSD(T), and CIS calculations were performed using Gaussian 94 (Revision E.6) and Gaussian 98

(Revision A.7)¹⁷ on Silicon Graphics O2 or Linux-based workstations. Minima and transition states were verified by the determination of vibrational frequencies. Convergence criteria for the geometry optimizations were that the RMS gradient was less than or equal to 3×10^{-4} and the maximum component of the gradient was less than or equal to 1.2×10^{-3} .

For the CASSCF and MRCI calculations, the software package MOLPRO¹⁸ running on Linux-based personal computers was employed. For the CASSCF and MRCI geometry optimizations, the convergence criteria were 3×10^{-4} for the RMS gradient and 5×10^{-4} for the maximum component of the gradient.

III. Results and Discussion

A. Ground Electronic State Calculations. Geometrical parameters for the global minimum of CHF₂ on the ground electronic surface are presented in Tables 1 and 2 at the MP2 and CCSD(T) levels of theory. The MP2/6-31G* values of Dearden et al.¹⁶ also are included for comparison. In agreement with previous theory and experiment,^{3,11,14,16} the lowest energy structure of CHF₂ is pyramidal with small H–C–F and F–C–F bond angles, which are close to the expected 109.5° for a sp³ hybridized carbon.

In comparing the geometries obtained from the MP2 and CCSD(T) methods for the ground electronic states, some trends are observed. First, little variation in either carbon–hydrogen or carbon–fluorine bond lengths is noted for all basis sets. At the MP2 level, variations of C–H bond lengths are less than 0.005 Å and C–F bond lengths vary by less than 0.011 Å. At

TABLE 3: Calculated Vibrational Frequencies^a for the Equilibrium Geometry of CHF₂ Using Various Basis Sets at the MP2 and CCSD(T) Levels of Theory

vibrational motion	sym	basis set					experiment
		6-31G* ^b	6-31+G*	6-311++G**	aug-cc-pVDZ	aug-cc-pVTZ	
MP2							
CF ₂ scissors	A	520	535	555	530	553	
OPLA bend	A	991	1078	1066	1045	1055	949 ± 10 ^b
CF ₂ sym stretch	A	1146	1168	1184	1144	1188	1164 ^c
CF ₂ asym stretch	A''	1177	1184	1203	1159	1305	1173 ^c
HCF def.	A''	1339	1362	1371	1328	1355	1317 ^c
CH stretch	A	2996	3238	3205	3201	3190	
CCSD(T)							
CF ₂ scissors	A	534	531	550	525		
OPLA bend	A	1061	1047	1036	1017		949 ± 10 ^b
CF ₂ sym stretch	A	1190	1160	1173	1135		1164 ^c
CF ₂ asym stretch	A''	1220	1182	1198	1156		1173 ^c
HCF def.	A''	1387	1346	1355	1316		1317 ^c
CH stretch	A	3159	3177	3159	3150		

^a All values are in cm⁻¹. ^b MP2(Full) results from Dearden et al.¹⁶ ^c Ar matrix values from Jacox.⁹

the CCSD(T) level, C–H bond lengths vary by less than 0.009 Å and C–F bond lengths vary by less than 0.018 Å. The C–F bonds tend to be slightly shorter by about 0.01 Å when triple- ζ quality basis sets are utilized. Second, H–C–F and F–C–F bond angles are also relatively insensitive to the level of theory, with variations for each angle of less than 0.3° across all basis sets and levels of theory.

Also shown in Tables 1 and 2 are the geometrical parameters for the transition structure for pyramidal inversion on the ground electronic state. As expected, the transition state is planar with C_{2v} symmetry. Once again, neither basis set nor level of theory has a significant effect on the bond lengths or angles. There are two structural changes of note upon formation of the planar structure. The first is a 6–9° increase in the H–C–F and F–C–F bond angles to around 120°. This increase is easily explained by simple VSEPR theory where ideal bond angles for a trigonal planar molecule are 120°. The second point is that across all basis sets and at both levels of theory there is a decrease of approximately 0.02 Å in the C–H bond length and a decrease of approximately 0.007 Å in the C–F bond length upon formation of the planar structure. This is because in the pyramidal structure the unpaired electron is located in a sp³ hybridized orbital on the central carbon. Thus, a significant portion of the electron–electron repulsion force vector lies along the C–H and C–F bond axis, slightly lengthening the bonds. In the planar structure the unpaired electron resides in a p orbital perpendicular to the C–H and C–F bond axis, effectively removing this extra repulsion term and shortening the bonds. As would be expected, the highly polar C–F bond is much less affected by this change than the more covalent C–H bond.

Also included in Tables 1 and 2 are the calculated barriers to pyramidal inversion. The barriers show only a minor basis set dependence of less than 350 cm⁻¹ at the MP2 level of theory and 150 cm⁻¹ at the CCSD(T) level. The calculated barrier energies at the CCSD(T) level are an additional 250–300 cm⁻¹ lower in energy than their MP2 counterparts. Of interest is the MP2 value of Dearden et al., obtained with the 6-31G* basis set, which is more than 330 cm⁻¹ higher than any of the results obtained in this work at the MP2 level of theory. This discrepancy is almost entirely due to Dearden et al. using uncorrected energies to calculate the barrier, while this work includes vibrational zero point energy corrections. Using the same 6-31G* basis set at the MP2 level, the result obtained for the uncorrected barrier is 3208 cm⁻¹, which is only 32 cm⁻¹ higher than the calculated value of Dearden et al. The remaining discrepancy is most likely due to the use of the frozen core

approximation in this work compared to the full MP2 calculation of Dearden et al.

The calculated barriers at both levels of theory tend to be smaller than, but within the error bars of, the experimental value of 2715 ± 400 cm⁻¹ found by Dearden et al. However, in their work, they used a computed C–H bond length of 1.0843 Å, a double well potential, and experimental data to derive the barrier height. Increasing the C–H bond length to the more accurate 1.0869 Å CCSD(T)/aug-cc-pVTZ value from this work would be expected to lower their measured barrier height slightly.

Vibrational frequencies of the ground-state equilibrium structure, calculated at the MP2 and CCSD(T) levels of theory, are listed in Table 3. The calculated MP2/6-31G* values of Dearden et al. also are listed for comparison, along with available experimental values. The calculated frequencies are in good agreement with experiment, particularly the values calculated at the CCSD(T) level of theory. The only exception is the out-of-plane bending mode, determined experimentally to have a frequency of 949 ± 10 cm⁻¹. Regardless of the level of theory and basis set, this mode is calculated to be too high by 7–15% in the present work, with the smallest difference between the experimental value and the CCSD(T)/aug-cc-pVTZ result. The large error for the out-of-plane bend is likely due to the more anharmonic nature of this vibration, which recently has been extensively investigated by Schwartz et al. in a QCISD/6-311G(d,p) study.¹⁴

B. Excited-State Results. 1. CIS Calculations. Preliminary investigations of the excited states of CHF₂ were initiated by calculating vertical excitation energies using the CIS method. The vertical excitation energies and oscillator strengths for transitions from the ground electronic state to the first three electronic excited states are reported in Table 4. Transition energies range from 61 355 to 71 372 cm⁻¹ depending on the identity of the upper state and the basis set used. Increasing the size of the basis set generally decreases the calculated transition energy. This is not surprising in that the larger basis sets, with the inclusion of additional diffuse and polarization functions, are better able to model the more diffuse excited states. Therefore, increasing the number of basis functions would be expected to lower the energy of the excited states at a faster rate than the corresponding ground-state energy. This in turn lowers the calculated vertical excitation energy. One other interesting point is that with the larger basis sets the gap between the first and second excited states increases from 5000 to 5600 cm⁻¹, whereas the gap between the second and third decreases from 2600 to 2100 cm⁻¹. Much of this difference is due to the

TABLE 4: Calculated Vertical Excitation Energies^a and Oscillator Strengths of the First Three Excited States of CHF₂ Using Various Basis Sets at the CIS Level of Theory

electronic state	6-31+G*		6-311++G**		aug-cc-pVDZ		aug-cc-pVTZ	
	energy	osc.	energy	osc.	energy	osc.	energy	osc.
\tilde{A}	64 065	0.031	62 532	0.028	62 250	0.029	61 355	0.028
\tilde{B}	68 226	0.015	67 880	0.012	67 162	0.010	66 944	0.010
\tilde{C}	71 372	0.003	70 573	0.002	69 485	0.003	69 065	0.003

^a All values are in cm⁻¹.

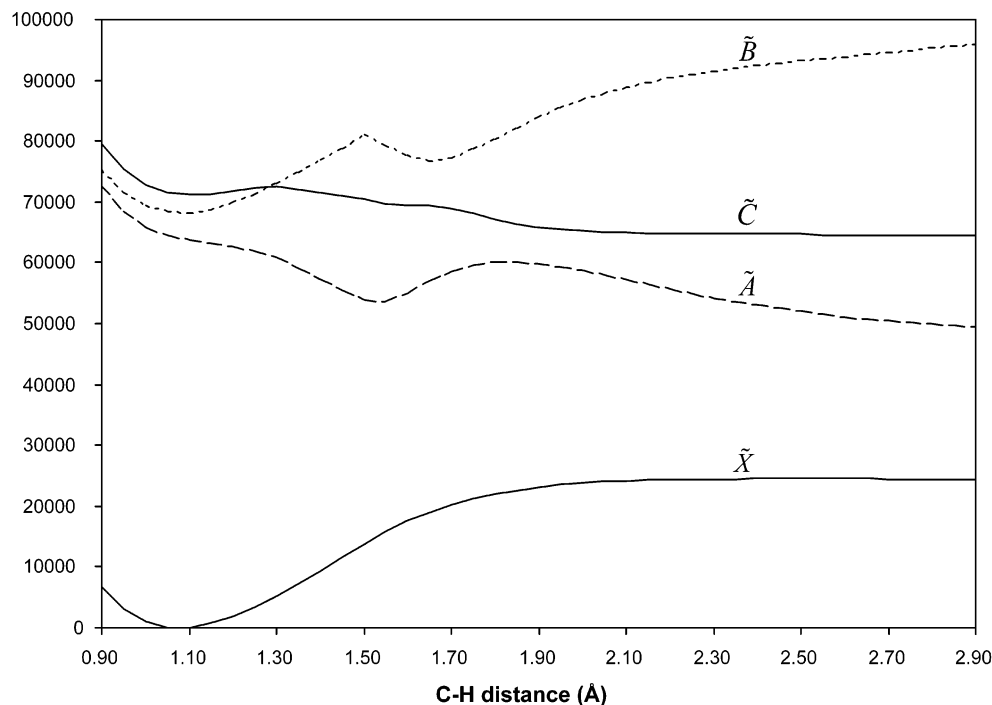


Figure 1. CIS/6-31+G* potential surface scan showing the ground and first three excited states of CHF₂. The C–H bond distance is varied in the scan, while the other coordinates were fixed at their equilibrium positions on the ground electronic surface.

fact that the second excited state is planar, meaning that a true vertical transition from the pyramidal ground state would end in a high vibrational level of the electronic excited state.

The first two excited states have been predicted to have unusually long C–H bonds by Dearden et al. To further characterize these states, potential surface scans were carried out in which the C–H bond distance was varied from approximately 0.9 Å to 4.0 Å with the C–F bond, the H–C–F and F–C–F angles, and the out-of-plane dihedral angle fixed at their equilibrium positions on the ground electronic surface. The CIS method was used to compute the energies of the excited states. The CIS/6-31+G* scans of the C–H bond for the ground and first three excited electronic states are shown in Figure 1.

From the C–H bond scans, it appears that starting from a nonplanar configuration, the first excited electronic state of CHF₂ does indeed have a rather long C–H bond, estimated to be around 1.7 Å at the CIS/6-31+G* level of theory. In addition, at this level of theory, the first excited state appears to be dissociative. The second excited state, which crosses with the third excited state at a C–H distance of about 1.3 Å, appears to have a minimum with a C–H bond distance of 1.1 Å as well as a second minimum with a C–H distance of about 1.7 Å. These first two excited-state surfaces were investigated in more detail using CASSCF and MRCI methods.

2. CASSCF and MRCI Calculations. The first excited electronic state of CHF₂ is expected to be nonplanar and have A' symmetry in the C_s point group. The \tilde{A} state is produced by excitation of the unpaired electron from the highest occupied

molecular orbital of the ground state, which has C–F π^* antibonding character. The unpaired electron is excited into an orbital that has significant antibonding character between the 2p_z-type atomic orbital on carbon and the 1s atomic orbital on hydrogen. This leads to a state predicted to have an unusually long C–H bond.¹⁶

CASSCF calculations were performed on the \tilde{A} state of CHF₂ using 19 active electrons in 13 orbitals, CASSCF(19,13). In addition, MRCI(3,4) calculations were also performed. The 6-31+G* and 6-311++G** basis sets were employed in all the calculations. Using standard geometry optimization techniques we were unable to locate an energy minimum for this state. To search for shallow minima on the potential energy surface, two-dimensional potential surface scans were carried out in which the C–H bond distance, the H–C–F bond angles, and the out-of-plane dihedral angle were varied.

A two-dimensional potential surface scan of the \tilde{A} state in which the C–H distance and the out-of-plane dihedral angle are varied is presented in Figure 2. In this scan, the C–F bonds are fixed at 1.30 Å, while the H–C–F bond angles are fixed at 115°. The scan at the CASSCF(19,13)/6-31+G* level shows what appears to be a minimum at a C–H distance of approximately 2.0 Å and a dihedral angle of greater than 148°. A scan obtained at the MRCI(3,4) level yields similar results, with an apparent minimum at a C–H distance of 2.0 Å and a dihedral angle of 144°.

With the C–H bond distance fixed at 2.0 Å and the C–F bond distance fixed at 1.30 Å, a two-dimensional scan of the

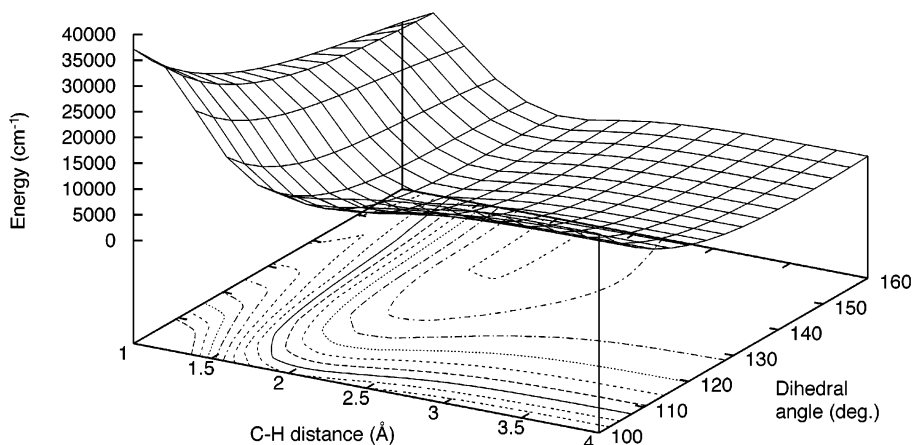


Figure 2. Two-dimensional potential surface scan of the first excited state of CHF_2 carried out using the CASSCF(19,13) method with the 6-31+G* basis set. The C–H bond distance and the out-of-plane dihedral angle were varied in the scan. The other coordinates were fixed at the following values: C–F distances, 1.30 Å; H–C–F angles, 115.0°. The lowest contour shown appears at 500 cm^{-1} and the contour spacing is 2000 cm^{-1} .

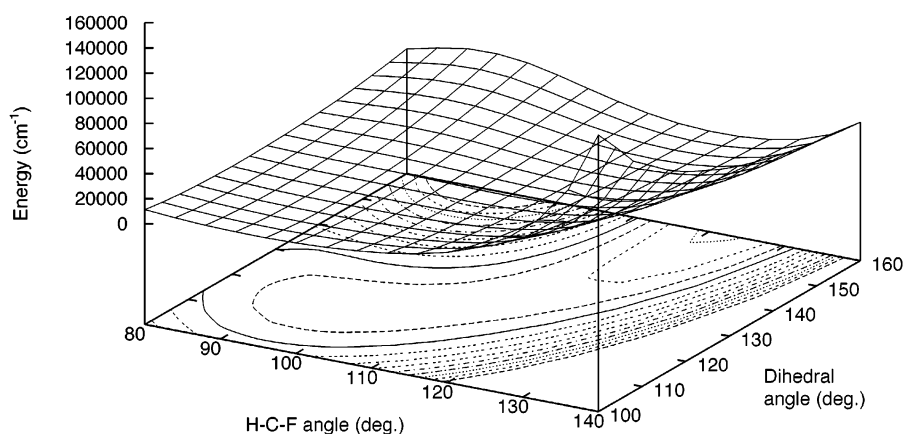


Figure 3. Two-dimensional potential surface scan of the first excited state of CHF_2 carried out using the CASSCF(19,13)/6-31+G* method. The H–C–F angles and the out-of-plane dihedral angle were varied in the scan. The other coordinates were fixed at the following values: C–H distance, 2.0 Å; C–F distances, 1.30 Å. The lowest contour shown appears at 500 cm^{-1} and the contour spacing is 2000 cm^{-1} .

TABLE 5: Results for the Second Excited State of CHF_2 (\tilde{B}) Obtained at the CASSCF and MRCI Levels of Theory

coordinate	CASSCF(19,13)/6-31+G*	CASSCF(19,13)/6-311++G**	MRCI(3,4)/6-31+G*
$r(\text{H}-\text{C})$, Å	1.0606	1.0606	1.0877
$r(\text{C}-\text{F})$, Å	1.4588	1.4501	1.4107
$\theta(\text{H}-\text{C}-\text{F})$, deg	133.89	133.71	132.24
$\theta(\text{F}-\text{C}-\text{F})$, deg	92.22	92.58	95.52
dihedral, deg	180.00	180.00	180.00
adiabatic transition energy, cm^{-1}	49 904	49 476	51 757

H–C–F angles and the out-of-plane dihedral angle was carried out and the result obtained at the CASSCF(19,13)/6-31+G* level is shown in Figure 3. Notice the broad low-energy channel stretching across the potential energy surface. A shallow local minimum with a well depth of approximately 130 cm^{-1} appears at an H–C–F angle of about 96° and a dihedral angle of 116°. This local minimum lies roughly 38 700 cm^{-1} above the ground-state minimum. Another deeper minimum with a well depth of about 3400 cm^{-1} seems to exist at an H–C–F angle of about 120° and a dihedral angle greater than 160° (probably corresponding to a planar or nearly planar configuration) and is 35 400 cm^{-1} above the ground-state minimum. Starting from the geometries of these two apparent minima, attempts to fully optimize the geometry of CHF_2 fail, presumably because of the shallow minima involved. The state indeed may be dissociative as the CIS calculations suggest.

The second excited electronic state of CHF_2 is expected to be planar and have A'' symmetry in the C_s point group (or A_1 symmetry in the C_{2v} point group). Unlike the situation for the

first excited state, geometry optimizations carried out on the second excited state were successful. Table 5 presents the equilibrium geometry of this state obtained at the CASSCF(19,13) and MRCI(3,4) levels of theory with 6-31+G* and 6-311++G** basis sets.

Contrary to the qualitative arguments presented by Dearden et al., the \tilde{B} state does not appear to have an unusually long C–H bond. In fact, the C–H bond of the optimized \tilde{B} state is calculated to be slightly shorter by 0.003–0.017 Å than the C–H bond of the ground state of CHF_2 . In addition, the C–F bond distance of the \tilde{B} state, computed to be 1.41–1.46 Å at all levels of theory, is elongated by more than 0.1 Å compared to the ground-state equilibrium bond length of 1.32–1.34 Å. The elongation of the C–F bonds is not surprising considering the quite small F–C–F angle of 92–96° computed for this state.

A two-dimensional potential surface scan of the \tilde{B} state of CHF_2 at the CASSCF(19,13)/6-31+G* level is presented in Figure 4. In this scan, the C–H bond distance was fixed at 1.06 Å and the C–F bond distance was fixed at 1.46 Å. The H–C–F

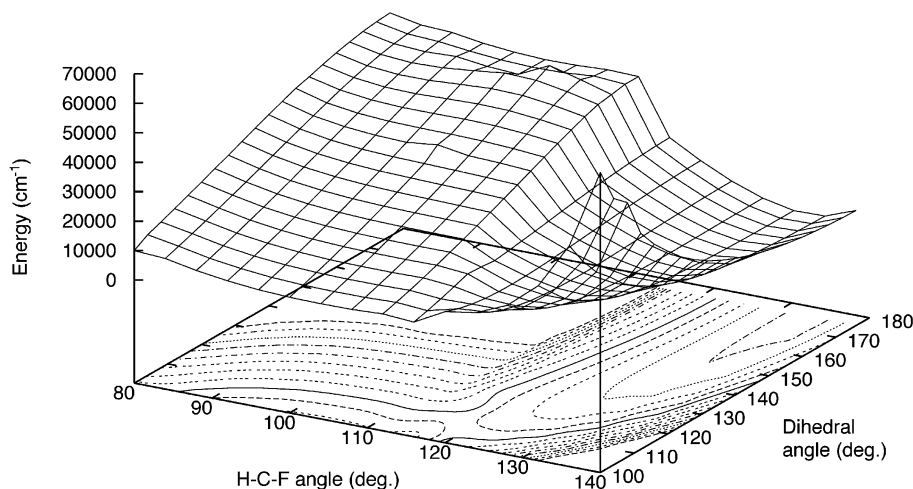


Figure 4. Two-dimensional potential surface scan of the second excited state of CHF₂ carried out using the CASSCF(19,13)/6-31+G* method. The H–C–F angles and the out-of-plane dihedral angle were varied in the scan. The other coordinates were fixed at the following values: C–H distance, 1.06 Å; C–F distances, 1.46 Å. The lowest contour shown appears at 500 cm⁻¹ and the contour spacing is 2000 cm⁻¹.

bond angles and the out-of-plane dihedral angle were varied to produce the potential surface scan. The scan clearly shows the minimum at planar geometries. In addition, the out-of-plane inversion vibration appears to be a fairly wide amplitude motion, with little energy required to bend the molecule out of the plane. For example, to bend the molecule 40° from its planar equilibrium configuration to a nonplanar structure with an out-of-plane dihedral angle of 140° requires only about 1800 cm⁻¹.

Also included in Table 5 are adiabatic transition energies for transitions from the nonplanar ground electronic state to the planar \tilde{B} state. The planar minimum on the \tilde{B} state surface of CHF₂ lies 49 500–51 800 cm⁻¹ above the ground-state minimum, depending on the level of theory and basis set. As mentioned previously, since the ground state is nonplanar and the second excited state is planar, the vertical excitation energies reported in Table 4 are much larger than the adiabatic transition energies because a vertical transition places the system higher up on the excited-state surface.

IV. Conclusions

The ground and first two excited electronic states of CHF₂ have been studied by using a variety of ab initio methods. The equilibrium geometry and pyramidal inversion transition state on the ground electronic surface were characterized by the MP2 and CCSD(T) levels of theory with a variety of basis sets. The equilibrium geometry is determined to be nonplanar in accord with previous work, with a computed barrier to pyramidal inversion of 2200–2800 cm⁻¹, depending on the level of theory and basis set. The barrier to inversion as well as vibrational frequencies of the equilibrium structure are in good agreement with previous experimental results.

The first two excited states of CHF₂ were investigated using the CIS, CASSCF, and MRCI methods. Potential surface scans of the first excited state show two possible local minima with shallow wells, both have long C–H bonds of about 2.0 Å: one is nonplanar with an H–C–F angle of approximately 96° and an out-of-plane dihedral angle of 116°; the other is planar or nearly planar with an H–C–F angle of about 120°. These minima lie 35 000–39 000 cm⁻¹ above the global minimum on the ground-state surface. However, attempts to optimize the geometry of the first excited state starting from the local minima fail; CIS calculations suggest that the state is possibly dissociative. Finally, the second excited electronic state, which lies

approximately 50 000 cm⁻¹ above the ground-state minimum, is determined to be planar with a long C–F bond of about 1.46 Å and a small F–C–F angle of about 92°.

Acknowledgment. Acknowledgment is made to the Illinois State University Research Grant program for support of portions of this work.

References and Notes

- (1) Molina, M. J.; Molina, L. T.; Kolb, C. E. *Annu. Rev. Phys. Chem.* **1996**, *47*, 327.
- (2) ATLAS 3 Public affairs status report #20, NASA Science Operations Marshall Space Flight Center, Huntsville, Nov. 13, 1994.
- (3) Francisco, J. S. *J. Phys. Chem. A* **2000**, *104*, 1499.
- (4) Maity, D. K.; Duncan, W. T.; Truong, T. N. *J. Phys. Chem. A* **1999**, *103*, 2152.
- (5) Olleta, A. C.; Lane, S. I. *Phys. Chem. Chem. Phys.* **2002**, *4*, 3341.
- (6) Schrader, D. M.; Karplus, M. *J. Chem. Phys.* **1964**, *40*, 1593.
- (7) Fessenden, R. W.; Schuler, R. H. *J. Chem. Phys.* **1965**, *43*, 2074.
- (8) Carver, T. G.; Andrews, L. *J. Chem. Phys.* **1969**, *50*, 5100.
- (9) Jacox, M. E. *J. Mol. Spectrosc.* **1980**, *81*, 349.
- (10) Chen, Y.; Tschuikow-Roux, E. *J. Phys. Chem.* **1993**, *97*, 3742.
- (11) Barone, V.; Grand, A.; Minichino, C.; Subra, R. *J. Chem. Phys.* **1993**, *99*, 6787.
- (12) Beiderhase, T.; Hack, W.; Hoyermann, K.; Olzmann, M. *Z. Phys. Chem.* **2000**, *214*, 625.
- (13) Nolte, J.; Wagner, H. G.; Temps, F.; Sears, T. J. *Ber. Bunsen-Ges.* **1997**, *101*, 1421.
- (14) Schwartz, M.; Peebles, L. R.; Berry, R. J.; Marshall, P. J. *J. Chem. Phys.* **2003**, *118*, 557.
- (15) McGivern, W. S.; Derecskei-Kovacs, A.; North, S. W.; Francisco, J. S. *J. Phys. Chem. A* **2000**, *104*, 436.
- (16) Dearden, D. V.; Hudgens, J. W.; Johnson III, R. D.; Tsai, B. P.; Kafafi, S. A. *J. Phys. Chem.* **1992**, *96*, 585.
- (17) Gaussian 98, Revision A.7, M. J. Frisch, G. W. Trucks, H. B. Schlegel, G. E. Scuseria, M. A. Robb, J. R. Cheeseman, V. G. Zakrzewski, J. A. Montgomery, Jr., R. E. Stratmann, J. C. Burant, S. Dapprich, J. M. Millam, A. D. Daniels, K. N. Kudin, M. C. Strain, O. Farkas, J. Tomasi, V. Barone, M. Cossi, R. Cammi, B. Mennucci, C. Pomelli, C. Adamo, S. Clifford, J. Ochterski, G. A. Petersson, P. Y. Ayala, Q. Cui, K. Morokuma, D. K. Malick, A. D. Rabuck, K. Ragavachari, J. B. Foresman, J. Cioslowski, J. V. Ortiz, A. G. Baboul, B. B. Stefanov, G. Liu, A. Liashenko, P. Piskorz, I. Komaromi, R. Gomperts, R. L. Martin, D. J. Fox, T. Keith, M. A. Al-Laham, C. Y. Peng, A. Nanayakkara, C. Gonzalez, M. Challacombe, P. M. W. Gill, B. Johnson, W. Chen, M. W. Wong, J. L. Andres, C. Gonzalez, M. Head-Gordon, E. S. Replogle, and J. A. Pople, Gaussian, Inc., Pittsburgh, PA, 1998.
- (18) Werner, H.-J.; Knowles, P. J.; Amos, R. D.; Bernhardsson, A.; Berning, A.; Celani, P.; Cooper, D. L.; Deegan, M. J. O.; Dobbyn, A. J.; Eckert, F.; Hampel, C.; Hetzer, G.; Korona, T.; Lindh, R.; Lloyd, A. W.; McNicholas, S. J.; Manby, F. R.; Meyer, W.; Mura, M. E.; Nicklass, A.; Palmieri, P.; Pitzer, R.; Rauhut, G.; Schütz, M.; Stoll, H.; Stone, A. J.; Tarroni, R.; Thorsteinsson, T. MOLPRO package of ab initio programs.